

Surface-enhanced Raman spectroscopy (SERS) substrate based on gold nanostars–silver nanostars for imidacloprid detection

Norhayati Abu Bakar^{A,B,*}  and Joseph George Shapter^A

For full list of author affiliations and declarations see end of paper

***Correspondence to:**

Norhayati Abu Bakar
Australian Institute for Bioengineering and Nanotechnology, University of Queensland, Saint Lucia, Brisbane, Qld 4072, Australia
Email: n.abubakar@uq.edu.au,
norhayati.ab@ukm.edu.my

Handling Editor:

Deanna D'Alessandro

Received: 2 October 2023
Accepted: 19 February 2024
Published: 4 April 2024

Cite this: Abu Bakar N and Shapter JG (2024) Surface-enhanced Raman spectroscopy (SERS) substrate based on gold nanostars–silver nanostars for imidacloprid detection. *Australian Journal of Chemistry* **77**, CH23189. doi:10.1071/CH23189

© 2024 The Author(s) (or their employer(s)). Published by CSIRO Publishing. This is an open access article distributed under the Creative Commons Attribution-NonCommercial-NoDerivatives 4.0 International License ([CC BY-NC-ND](https://creativecommons.org/licenses/by-nc-nd/4.0/))

OPEN ACCESS

ABSTRACT

Surface-enhanced Raman spectroscopy (SERS) is a powerful molecular spectroscopy technique that combines Raman spectroscopy with nanostructured metallic surfaces to amplify the Raman signals of target molecules by more than 10^3 . The high sensitivity of SERS poses a significant opportunity for pesticide detection in complex matrices at ultralow concentrations. In this study, we improved the SERS sensitivity for imidacloprid (IMD) by employing silver nanostars (AgNs) coated with gold nanostars (AuNs) as the SERS-active substrate. The SERS response towards IMD detection increased based on the combination of AuNs and AgNs on the substrate surface. The intensity of the SERS signal of IMD using the AuNs/AgNs substrate increased compared to using individual metal nanoparticle substrates. The excellent reproducibility of SERS intensity using the AuNs/AgNs substrate was achieved with a low relative standard derivative (RSD) of 4.87% for 20 different spots on the same sample and 5.19% for 20 different samples. This detection system can be used for multiple tests, which is crucial for the advancement of handheld sensors designed for field use, where minimal or no high-level technical support is accessible.

Keywords: bimetallic nanostructures, gold nanostars, imidacloprid, neonicotinoid pesticides, silver nanostars, surface plasmonic sensors, surface-enhanced Raman scattering, thin film.

Introduction

Global food insecurity is a significant concern when the estimated global yield loss for crop production is ~20–40% annually due to crop pathogens and insect pests.¹ Additionally, the impact of climate change and the outbreak of plant diseases has increased the pressure in the agricultural sector to meet the demands of population growth. Consequently, there has been a growing requirement for implementing fast and efficient pest control in farming practices. Imidacloprid (IMD) is a new and modern potent insecticide with high insecticidal efficiency against sucking insects and is commonly used in soil injection, seed treatments and foliar spray. The demand for IMD has been rapidly increasing and it is applied globally in agricultural practice mainly to control aphids, leafhoppers, thrips, whiteflies and termites on crop.² Unfortunately, most chemical pesticides pose risks to humans and the environment due to their essential toxicity to pests. They persist for long periods of time in the environment and can accumulate and pass from one species to the next through the food chain. Owing to its persistence and high solubility in water systems, IMD residue has been found in water and soil in the United States of America, Canada, Australia, China and Europe.³ The highest IMD residue level in water samples has been recorded as 37% after collecting from 48 streams across the USA.⁴ Unfortunately, IMD has been found in food chain systems with its residue having been detected in soil,⁵ milk,⁶ fruit and vegetables.⁷

Surface-enhanced Raman spectroscopy (SERS) is an accurate and sensitive analytical tool for detecting and identifying trace amounts of various chemicals. This is a powerful molecular spectroscopy technique that combines Raman spectroscopy with nanostructured metallic surfaces to amplify the Raman signals of target molecules. The SERS intensity of the molecule detection can be enhanced by more than 10^3 depending on

the metal nanoparticles' materials and their geometries on the substrate surfaces.^{8–14} This enormous enhancement of SERS intensity allows the detection of chemical hazards in agricultural products at very low concentrations and in complex matrices. The ability to monitor ultralow concentrations of agricultural products such as pesticides in the environment and in food is critical, as governments have regulated maximum residue limits for farmer use and banned dangerous pesticides. Conventional methods used for pesticide detection include liquid chromatography–mass spectroscopy (LC-MS),¹⁵ gas chromatography–mass spectroscopy (GC-MS),¹⁶ fluorescence,¹⁷ enzyme-linked immunoabsorbent assays¹⁸ and capillary electrophoresis.¹⁹ However, these analytical techniques are costly, require significant labor and time investment, rely on sophisticated instruments and depend on skilled staff. Unfortunately, many developing countries lack the financial resources to afford such expensive instruments or have limited access to adequate equipment for monitoring pesticide residue in food or the environment. Nowadays, the SERS technique has been established for the detection of pesticide residues through numerous published articles due to its quick response, facile use and high accuracy. Moreover, SERS-active substrates are readily integrated into analytical systems for portable SERS analysis for use in the field and outside research labs.

Metallic SERS substrates have been fabricated to create powerful detectors for identifying tiny amounts of chemicals, even in complicated matrices. The fabrication of straightforward, reproducible, reusable devices plays a crucial role for the Raman amplification of the analyte after absorption on the metallic surface. The most common metal nanoparticles used in SERS sensing are gold and silver nanoparticles. Gold has become a very popular metallic material because it is easily stabilised due to its chemical, biocompatible and bioinert properties.²⁰ Silver has also been extensively employed as a SERS substrate because it has a sufficiently long shelf-life and is stable after deposition on a solid surface and reported widely to have a large electromagnetic enhancement.²¹ The parameters are continuing to be explored in SERS substrate fabrication by combining the two most used plasmonic nanostructures in order to optimise the enhancement of Raman scattering and produce stable SERS-active substrates that are not susceptible to surface oxidation.²² It also has been found that bimetallic nanoparticles consistently exhibit very high SERS enhancement, and improve the selectivity and enhance the capture of the analyte on the plasmonic surface.²³

Inspired by this work, we introduced gold nanostars (AuNs) on silver nanostar (AgNs) surfaces to increase the SERS response towards IMD. To date there are no reports of SERS detection of IMD using bimetallic AuNs/AgNs assemblies. This combination of two metal nanostars proved to be an outstanding SERS substrate due to the very rough surface, which led to a large electromagnetic field enhancement from

lots of hotspots. We also observed the monometallic AuNs and AgNs systems towards IMD detection in order to determine the optimum SERS substrate for monitoring of the pesticides. We believe this SERS result has opened the door to future monitoring of food or environment contaminations and could be readily integrated into analytical systems for portable SERS analysis.

Results and discussion

We studied the formation of colloidal AgNs, AuNs and the combination of AuNs/AgNs using optical and structure characterisations. Transmission electron microscopy (TEM) images showed the successful formation of AgNs (Fig. 1a) and AuNs (Fig. 1b) in the colloidal phase. TEM images and energy-dispersive X-ray spectroscopy (EDS) analysis demonstrated that the AuNs particles surrounded the surface of the AgNs particles (Fig. 1d–g) after both colloids were mixed in a 1-to-1 volume ratio. The concentrations of the AuNs and AgNs dispersions were found to be respectively 9.1×10^{-10} and 5×10^{-12} M using the Beer–Lambert Law and reported values of the extinction coefficients for the species.^{24,25} It was found that AuNs with an average diameter 30 nm coated the bodies and arms of the AgNs' surface as observed in Fig. 1d. The image in Fig. 1e is an overlay of a scanning transmission electron microscopy (STEM) image showing that the two elements present in the AuNs/AgNs surface are silver (Ag) and gold (Au). Fig. 1f is an elemental map of Ag and Fig. 1g is an elemental map of Au. The EDS analysis for gold and silver is available in Supplementary Fig. S1. The structure of the hybrid is not surprising as the higher concentration of the AuNs will provide more than enough material to completely coat the much larger AgNs nanoparticles. The remarkable changes in absorbance spectra in Fig. 1c are in agreement with the TEM images and EDS analysis, showing the plasmon resonance of AuNs/AgNs arising in the range from 350 to 600 nm. The higher absorbance feature closest to 380 nm is predominant, explaining that the main combination to plasmon resonance comes from the silver nanostar particles.

The morphology and optical absorbance of the AuNs, AgNs and AuNs/AgNs film surfaces were characterised using a JOEL JSM-7100F FESEM and UV-2600 Shimadzu. Star-shaped AgNs with long tips were successfully deposited on the surface (Fig. 2a) and agglomerated star-shaped gold nanoparticles were deposited on the substrate surface (Fig. 2b). Moreover, the AuNs/AgNs thin film surface displayed a good distribution of AuNs/AgNs particles on the silicon surface (Fig. 2c). The majority of the tips and branches of the AgNs can still be seen after the presence of AuNs on the AgNs surface. As observed in Fig. 2d, EDS analysis reports a good percentage of gold detected on the AuNs/AgNs surface. The saturation coverage of the AgNs did not require all the AuNs in the dispersion and hence the

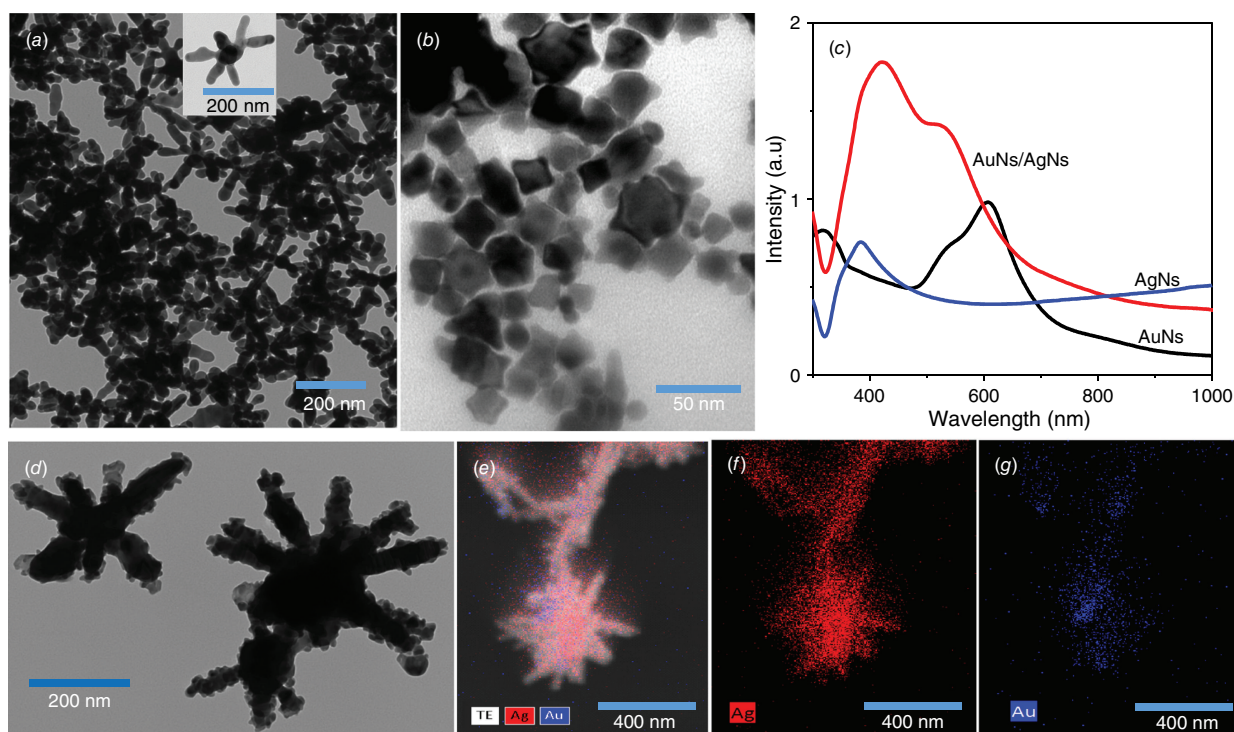


Fig. 1. Colloidal particles: (a) TEM image of AgNs and (b) TEM image of AuNs. (c) Absorbance of AgNs, AuNs and AuNs/AgNs. (d–g) TEM image and STEM analysis of the AuNs/AgNs.

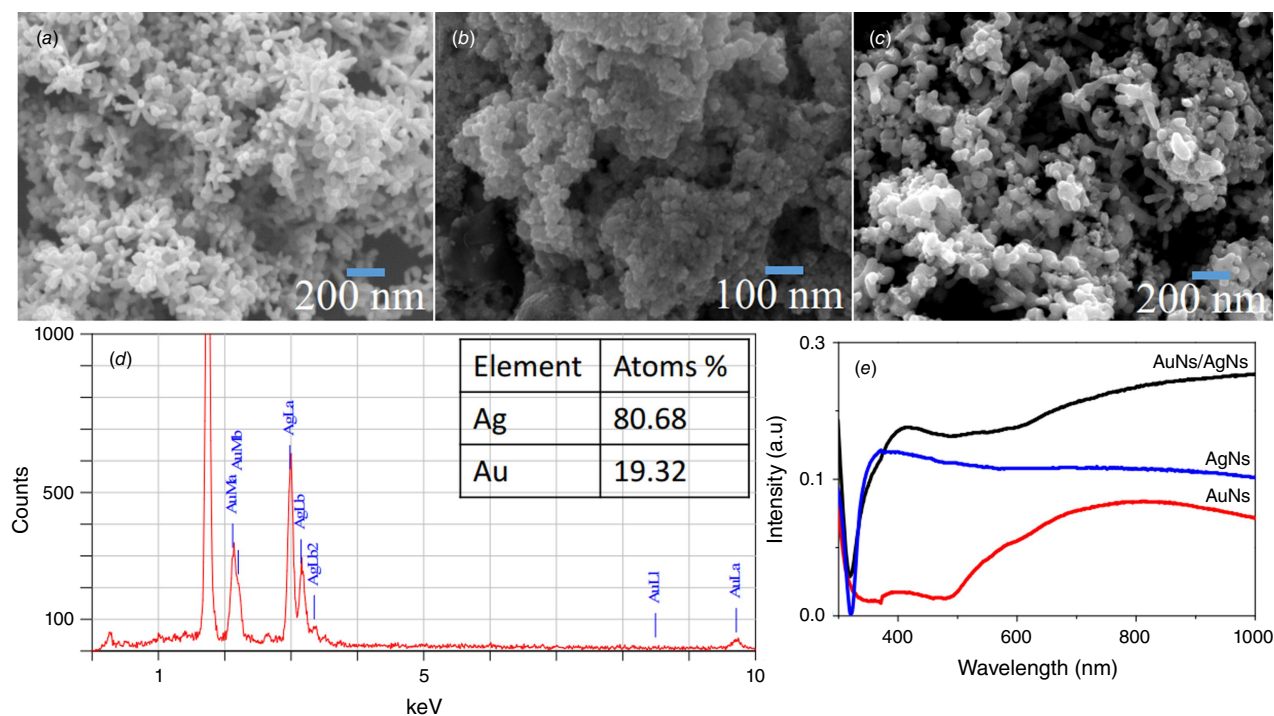


Fig. 2. Thin films characterisations: (a) SEM image of AgNs, (b) SEM image of AuNs, (c) SEM image of the AuNs/AgNs, (d) atomic percentage of the AuNs/AgNs substrate and (e) absorbance of AgNs, AuNs and AuNs/AgNs films.

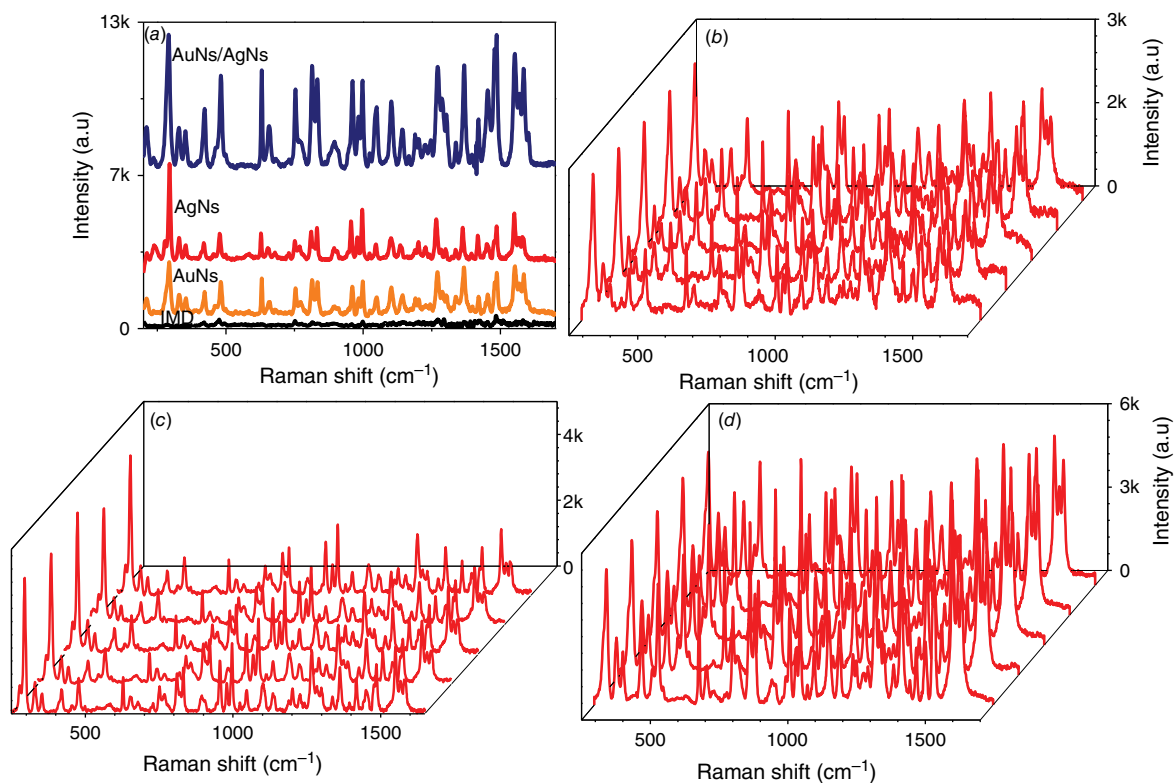


Fig. 3. SERS measurements of 1 mg mL^{-1} IMD: (a) SERS signals on bare glass, AuNs, AgNs and AuNs/AgNs surfaces, (b) SERS signals on AuNs for five different spots, (c) SERS signals on AgNs for five different spots and (d) SERS signals on AuNs/AgNs for five different spots.

ratio of Ag to Au in the adsorbed hybrid is higher than the ratio of the species in the component dispersions. The absorbance spectra of the AuNs/AgNs thin film in Fig. 2e confirmed the existence of the AuNs surrounding the AgNs. The UV-Vis spectrum of the AuNs/AgNs combination is essentially the addition of two individual spectra.

To evaluate the sensitivity of AgNs, AuNs and AuNs/AgNs SERS substrates towards IMD detection, 1 mg mL^{-1} of IMD was dropped and dried on each SERS substrate and a bare glass surface. The presence of IMD on the SERS-active substrate surfaces was confirmed by the existence of characteristic peaks of IMD that matched the corresponding bands of IMD on the glass surface. The vibrational assignment for the SERS signal of IMD is provided in Supplementary Table S1. We observed that the intensity of the IMD peaks clearly increased after the absorption of IMD on the AuNs, AgNs and AuNs/AgNs surfaces, as shown in Fig. 3a. The intensity of the SERS spectra of IMD on individual AgNs and AuNs surfaces is very similar. However, the combination of AgNs and AuNs on the substrate surface increased the SERS sensitivity for IMD detection. The spectra for the AuNs and the hybrid are very similar due to the structure of the hybrid where the outermost component of the hybrid is largely AuNs (see Fig. 1d) leading to adsorption of IMD on AuNs in both cases. In order to further evaluate the

sensitivity performance of these SERS substrates towards IMD detection, one of the highest peaks at 1486 cm^{-1} , which was assigned to the C–H bending, was chosen to calculate the enhancement factor (EF) value. The calculated EF values for the AgNs, AuNs and AuNs/AgNs substrates are 4.34×10^4 , 4.32×10^4 and 1.36×10^5 respectively. This result indicates the combination of these nanoparticles on the substrate surface showed a higher SERS response towards IMD detection by increasing the active SERS locations around the bimetallic particles.

The detection reproducibility of 1 mg mL^{-1} IMD was studied on AgNs, AuNs and AuNs/AgNs substrate surfaces by taking SERS measurements on 20 different spots on the same sample. The full SERS spectra are provided in Supplementary Fig. S2. Fig. 3b–d shows five spectra from different spots on each of the SERS substrate surfaces. We observed the three highest intensity characteristic peaks at 811 , 1486 and 1552 cm^{-1} for each substrate to calculate the relative standard deviation (RSD) and analyse the uniformity of the field enhancement of the SERS substrate. Based on the RSD results in Supplementary Fig. S3, the AuNs and AuNs/AgNs substrate surfaces show good local field enhancements for SERS detection of IMD, with uniform enhancement. The lowest and the highest RSD value for the AuNs surface were ~ 4.38 and 5.89% , whereas for the AuNs/AgNs substrate they

are 4.87 and 6.59%. By contrast, the calculated RSD value for the AgNs surface is higher than the AuNs and AuNs/AgNs surfaces showing the lowest and highest RSD at 7.07 and 12.63%.

We also explored the reproducibility of IMD detection on 20 different samples of each SERS substrate; the 20 full spectra are provided in Supplementary Fig. S4. Fig. 4 shows five spectra from different SERS substrates. From these 20 spectra, we calculated the uniformity of field enhancement by measuring the RSD value for each substrate. The three highest intensity characteristic peaks at 811, 1486 and 1552 cm^{-1} were used for RSD calculation. The RSD graphs are provided in Supplementary Fig. S5. For the AuNs substrate, the highest and lowest RSD values were 14.31 and 8.05%. This is much lower than the highest and lowest RSD values for AgNs, which were ~ 18.23 and 8.66%. However, the AuNs/AgNs substrate showed good local field enhancements for SERS detection of IMD by exhibiting uniform inherent field enhancement, with highest and lowest RSD values of 5.89 and 6.59%.

In order to further observe the sensitivity performance of the AuNs/AgNs SERS substrate, seven IMD concentrations were absorbed on the AgNs, AuNs and AuNs/AgNs surfaces. Fig. 5 shows the corresponding SERS spectra of different IMD concentrations ranging from 1 ng mL^{-1} to 1 mg mL^{-1} . It was found that IMD can be detected using AuNs, AgNs and

AuNs/AgNs substrates at a concentration as low as 1 ng mL^{-1} by giving clear strong SERS features. The SERS intensity significantly decreased with the decrease of the IMD concentrations on the SERS surface as expected. By comparison, IMD signals on the bimetallic particle surface were much higher than those signals on the individual AuNs and AgNs surfaces for the seven IMD concentrations. However, the characteristic peaks of the pesticide at its lowest concentration on the AuNs and AgNs surfaces are still observable. We further studied the limit of detection (LOD) of the SERS substrates based on the three highest peaks of IMD by plotting the log relationship between SERS intensity and concentrations of IMD. Fig. 6 shows the corresponding log relationship of SERS intensity and seven IMD concentrations. We found that the log relationship for the bimetallic substrate has a good correlation as high as 0.98 for the band at 1486 cm^{-1} compared to the AuNs and AgNs surfaces. These good correlations for IMD pesticide show that the SERS substrates could be used to estimate residual pesticide levels in the environment and food products. Using a signal to noise ratio of 3 to 1, the LOD for IMD were determined and found to be 2.4×10^{-6} mg mL^{-1} on the AuNs surface, 2.5×10^{-7} mg mL^{-1} on the AgNs surface and 5.5×10^{-8} mg mL^{-1} on the AuNs/AgNs surface.

We have also assessed the reusability of our substrates, which involves utilising the same substrate multiple times.

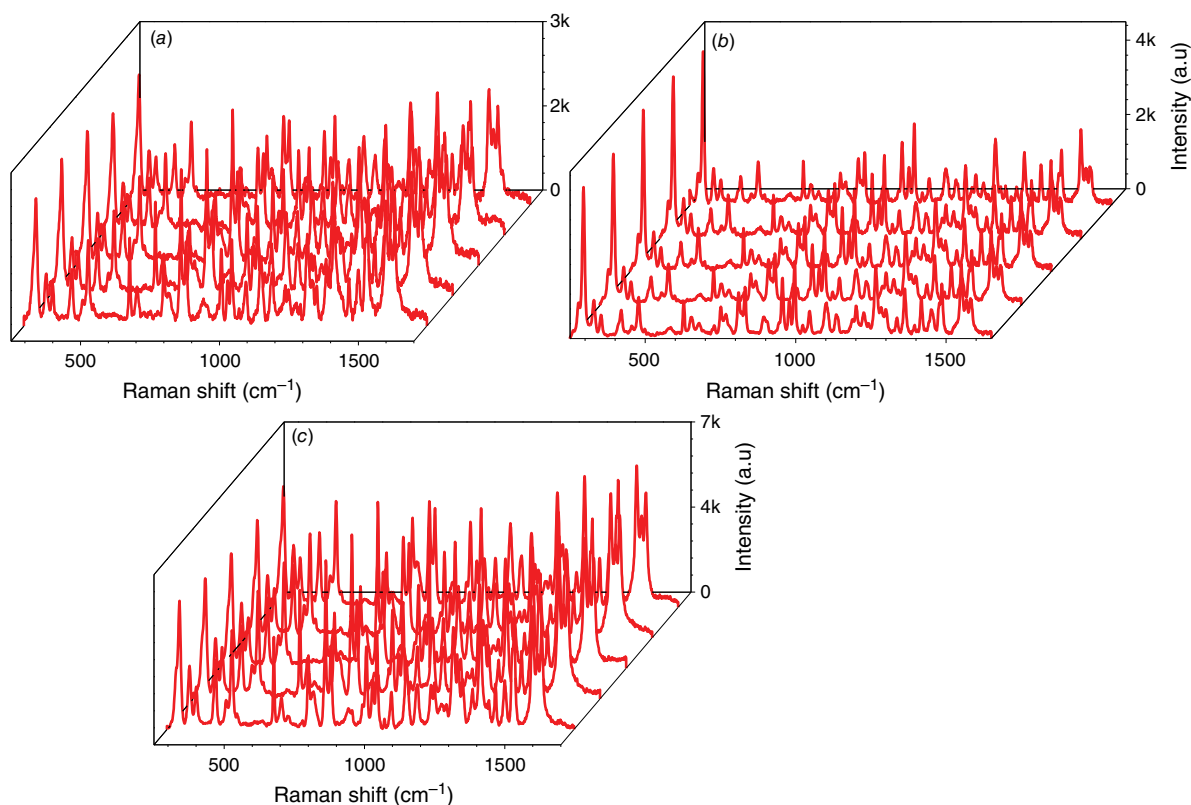


Fig. 4. SERS measurements of 1 mg mL^{-1} IMD: (a) SERS signals on the AuNs surface for five different samples, (b) SERS signals on the AgNs surface for five different samples and (c) SERS signals on the AuNs/AgNs surface for five different samples.

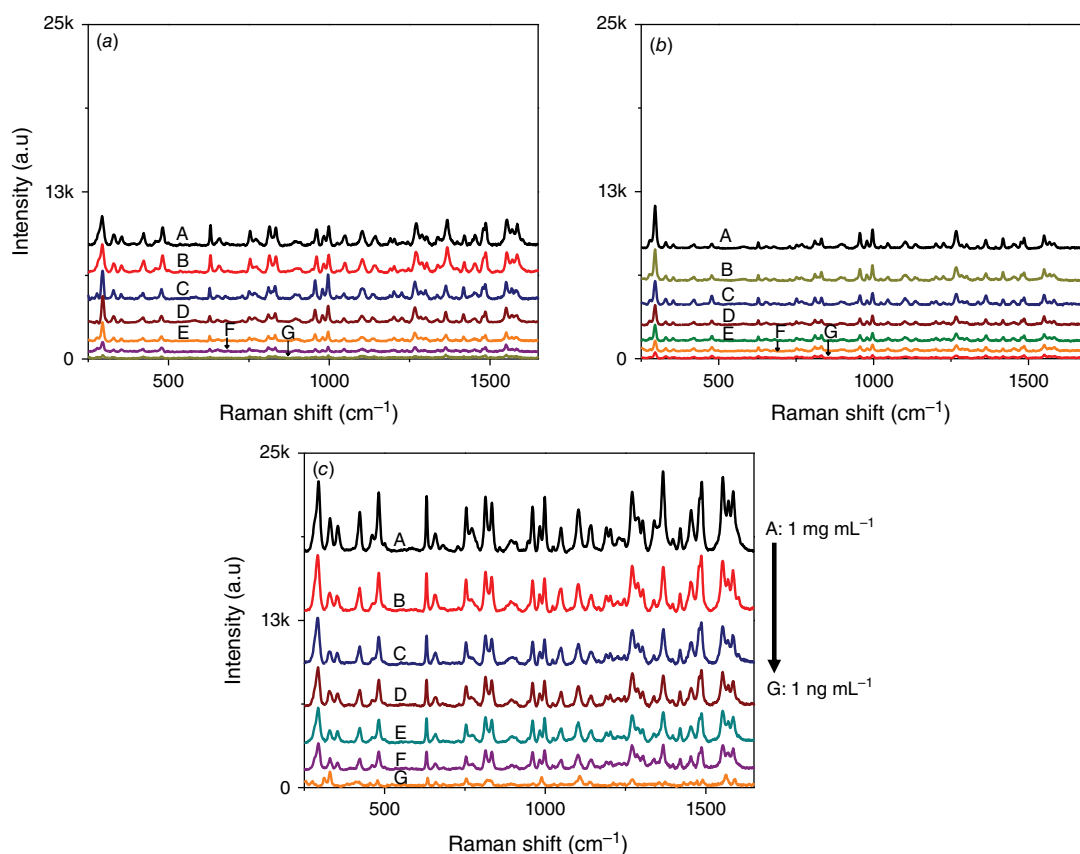


Fig. 5. IMD signals of seven concentrations on (a) AuNs, (b) AgNs and (c) AuNs/AgNs surfaces.

An essential aspect of any detection system is its capability to be used in multiple tests. This evaluation is crucial for the development of a sensor intended for field use, typically operated by staff with minimal training. To examine the reusability performance of the SERS substrate, we recorded the Raman spectrum of the bare metal nanostars films, the SERS spectrum of IMD on metal nanostars films and the Raman spectrum of the metal nanostars (bare again) after the removal of IMD from the metal nanostars surface across five cycles, as depicted in Fig. 7. The reusability procedure involved using the SERS substrates as outlined and then cleaning them by washing with ethanol to eliminate the adsorbed pesticide. The removal of the pesticide was confirmed by recording the Raman signal of the bare film. Subsequently, the same concentration of pesticide was added to the film surface and a SERS spectrum of the pesticide once again measured. Over five cycles, there is minimal degradation in the observed SERS signal, confirming the substrate's robustness. SEM images of the substrates after five cycles of detection and washing are provided in Supplementary Fig. S6 and confirm minimal changes throughout the cycling process. The thickness of the metal nanostars coverage ensures that the available active components undergo minimal changes, leading to consistent SERS performance. In addition, the EDS analysis agrees with the

SEM images confirming a slight reduction of $\sim 3\%$ in the percentage of gold after five cycles of the washing process for the AuNs/AgNs surface.

Following a storage period of 1 month in a small transparent container with silica gel, the AuNs, AgNs and AuNs/AgNs films exhibited the same SERS intensity as newly prepared metal nanostars films. Fig. 8 illustrates the corresponding SERS intensity of the three characteristic peaks of IMD at 811, 1486 and 1552 cm^{-1} for each substrate over a month. The IMD signals appeared to decrease slightly over time, however the decrease in the RSD value for the SERS signals remains low. For the AuNs substrate, the highest and lowest RSD values were 8.59 and 3.81%. By contrast, the highest and lowest RSD values for the AgNs substrate were ~ 3.27 and 2.33%. Notably, the AuNs/AgNs surface exhibited strong stability, with the highest and lowest calculated RSD values being 3.73 and 2.16%. The stable SERS spectra of IMD on the SERS substrates and the RSD for the three characteristic peaks are provided in Supplementary Figs S7 and S8.

Early work to detect IMD with SERS was successful but gave poor sensitivity.^{26,27} More recently, the utilisation of Ag nanoparticles for IMD detection has been observed with silver nanoflowers²⁸ or a gold coated silver nanoflower SERS substrate.²⁹ The work with silver nanoflowers gave a LOD of

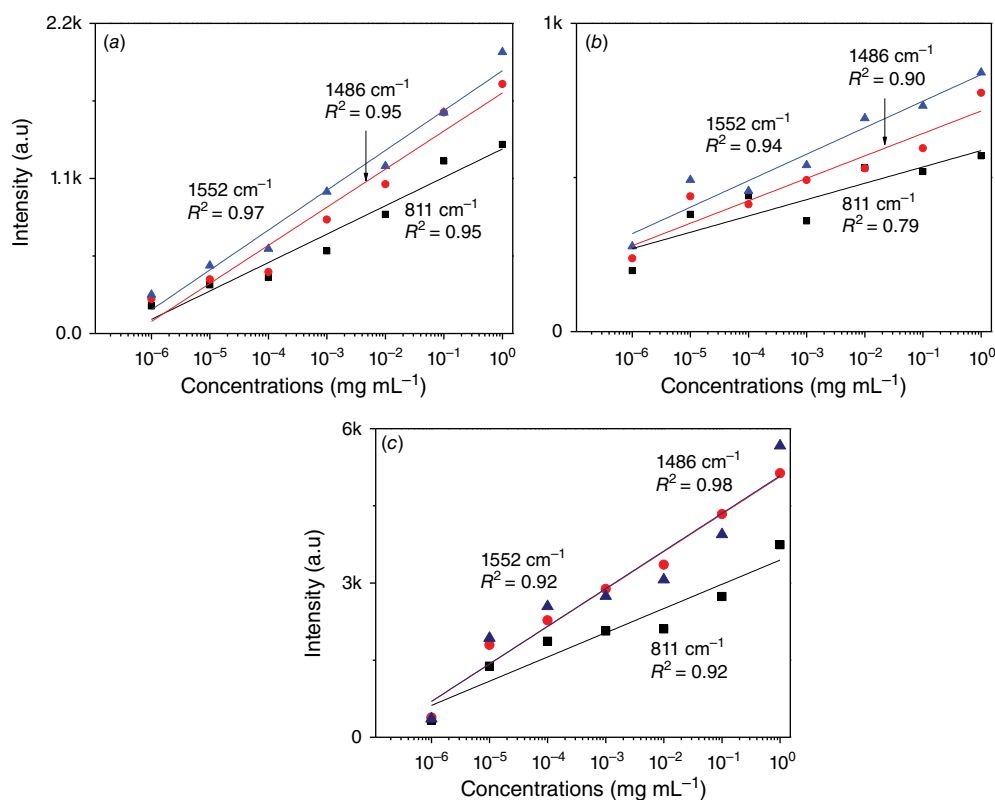


Fig. 6. Log concentration relationship of IMD signals versus concentrations on (a) AuNs, (b) AgNs and (c) AuNs/AgNs substrates.

$4.55 \times 10^{-5} \mu\text{g mL}^{-1}$, which is similar to the sensitivity observed in this work using AuNs/AgNs in terms of the LODs for IMD employing SERS substrates. The introduction of gold to silver nanoflowers has been demonstrated to enhance the sensitivity by a factor of ~ 100 . This led to observed LODs of $4.25 \times 10^{-10} \text{ mg mL}^{-1}$. Other recent studies have utilised roughened silver³⁰ and palladium nanoparticles on mesoporous silicon³¹ as SERS substrates, demonstrating very similar LODs for IMD (LODs of 1×10^{-6} and $2.55 \times 10^{-7} \text{ mg mL}^{-1}$). A combination of gold and silver nanoparticles has been reported to detect IMD with a LOD of $0.0128 \text{ mg mL}^{-1}$.³² In our work, the LOD of IMD on the AuNs surface is $2.4 \times 10^{-6} \text{ mg mL}^{-1}$, AgNs surface is $2.5 \times 10^{-7} \text{ mg mL}^{-1}$ and AuNs/AgNs surface is $5.5 \times 10^{-8} \text{ mg mL}^{-1}$, which is an improvement on most of the sensitivities reported previously. Importantly, our work is the first to demonstrate the potential to reuse the active substrate many times, which will be critical for commercial applications. Our project findings hold practical significance for estimating IMD residue in food products, as the LOD is notably lower than the current concentrations permissible set by the Chinese government for fruit, ranging from 1.91 to $3.91 \mu\text{mol L}^{-1}$ (equivalent to 4.89×10^{-4} – $10.0 \times 10^{-4} \text{ mg mL}^{-1}$), as well as the limit set by the European Union at 0.5 mg kg^{-1} (equivalent to $5 \times 10^{-4} \text{ mg mL}^{-1}$).³³

Conclusions

In summary, we have developed a new SERS substrate as a straightforward detector for sensing the pesticide IMD at low concentrations, achieved by combining two types of metal nanostars on a substrate surface. The sensor effectively assessed IMD concentrations with a LOD of less than 1 ng mL^{-1} . The results indicate an enhancement in IMD signal at low concentrations on the AuNs/AgNs surface when compared to the signal on a surface composed of a single type of metal nanostar. The SERS measurements conducted for IMD detection demonstrated that the AuNs/AgNs SERS substrates exhibited high sensitivity and good reproducibility and stability and can be used multiple times for pesticide detection. Therefore, we believe this combination of AgNs and AuNs as a SERS substrate has promising future applications in food and environment sensing.

Experimental

The preparation of gold nanostars using the one-pot synthesis method was adapted from Batmunkh *et al.*³⁴ The chemicals used in the AuNs colloidal synthesis were gold(III) chloride trihydrate ($\text{HAuCl}_3 \cdot 3\text{H}_2\text{O}$) ($\geq 99.9\%$, Sigma–Aldrich),

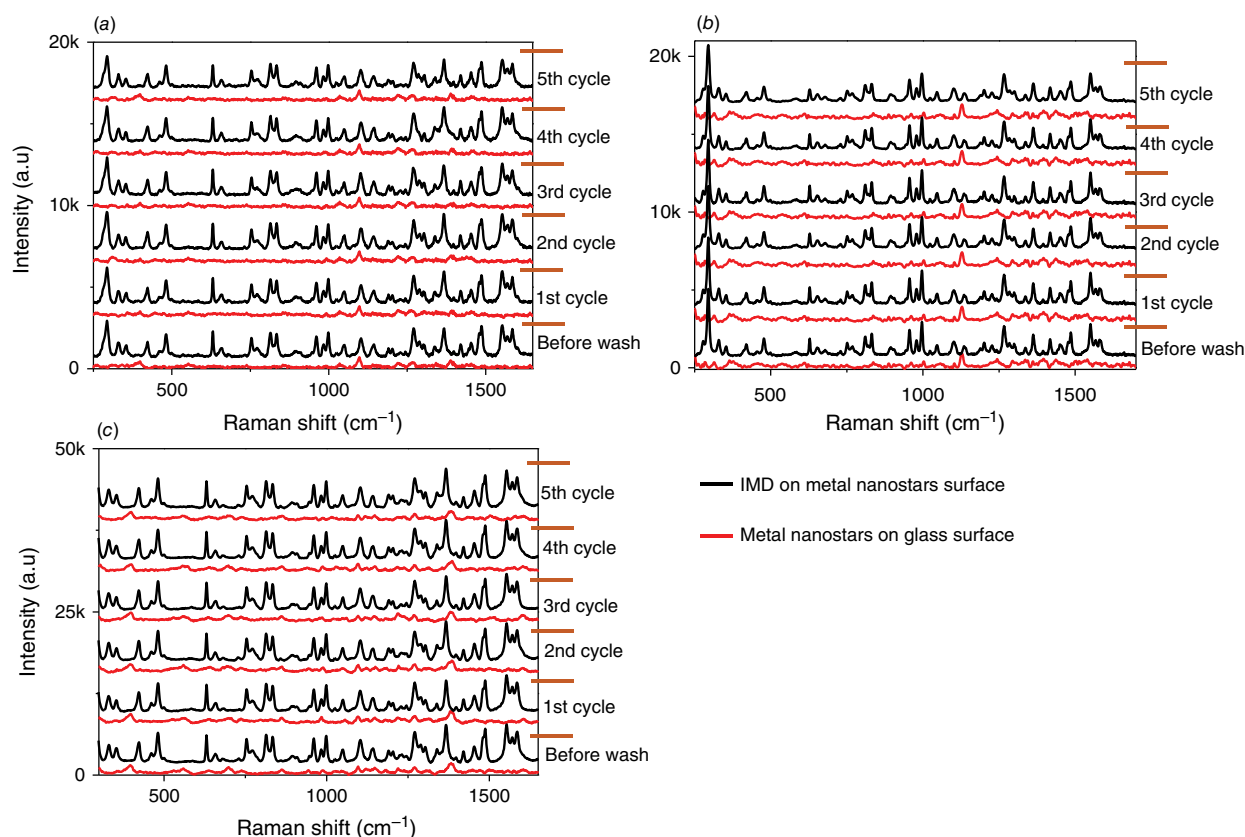


Fig. 7. Reusability performance towards IMD detection for (a) AuNs, (b) AgNs and (c) AuNs/AgNs substrates.

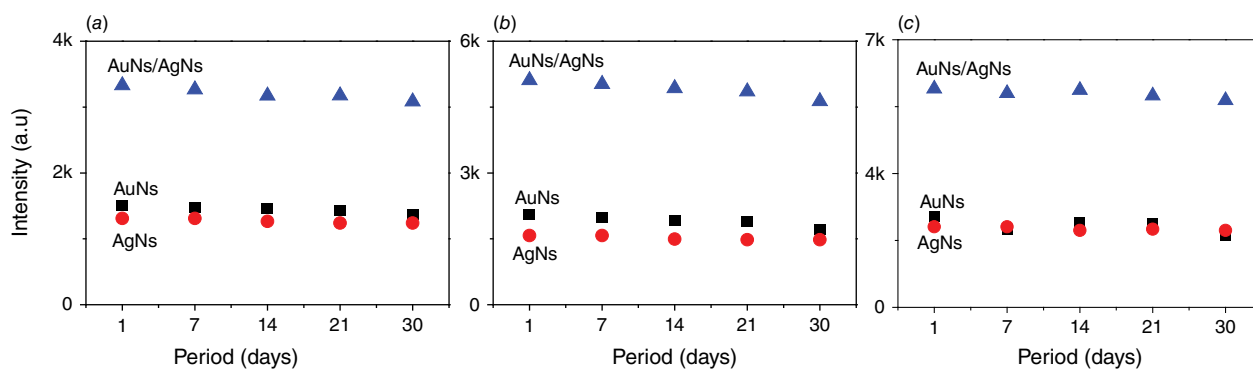


Fig. 8. The stability SERS spectra of IMD signals at (a) 811 cm^{-1} , (b) 1486 cm^{-1} and (c) 1552 cm^{-1} peaks.

4-(2-hydroxyethyl)piperazine-1-ethanesulfonic acid (HEPES), ($\geq 99.5\%$ (titration), Sigma-Aldrich) and sodium hydroxide (NaOH) ($\geq 98.0\%$, Chem-Supply Pty Ltd). A typical AuNs preparation started by preparing 10 mL of 100 mM HEPES at pH 7 by adding 0.2 mL of 1 M NaOH. Subsequently, 2 mL of the solution was mixed with 3 mL of water. Finally, 0.05 mL of 20 mM $\text{HAuCl}_4 \cdot 3\text{H}_2\text{O}$ was added to the solution. After 30 min, the clear colourless solution changed to a blue colour. The AuNs colloids were washed using ethanol by centrifugation using an Allegra X-22 centrifuge (Beckman Coulter) at 6000 rpm for 15 min at room temperature. The

pellet was collected, dissolved in water and further used for AuNs and AuNs/AgNs thin film fabrication.

The preparation of AgNs colloids and the fabrication of a AgNs thin film on glass and silicon surfaces using a self-assembly technique have been reported in our previous article.³⁵ The fabrication of AuNs thin films and AuNs/AgNs thin films was performed using the same method for the AgNs thin films. The AuNs/AgNs colloids were prepared by mixing equal volumes of the AuNs and AgNs colloid dispersions. This colloid mixture was further used to fabricate AuNs/AgNs thin films using the self-assembly technique.

Seven concentrations of IMD pesticide at 1×10^0 , 1×10^{-1} , 1×10^{-2} , 1×10^{-3} , 1×10^{-4} , 1×10^{-5} and 1×10^{-6} mg mL⁻¹ were prepared to study the performance of AgNs, AuNs and AuNs/AgNs thin films as SERS substrates. The SERS measurements for pesticide detection were performed using a Renishaw model InVia micro Raman spectrometer with a 785-nm wavelength diode laser at 1% of a 167-mW power laser. The reference spectrum of IMD on bare glass and SERS spectra were collected at 1% of a 167-mW power laser using a 50× objective with five accumulations. SERS sensor properties such as sensitivity, reproducibility, reusability and stability towards the pesticide detection using AgNs, AuNs and AuNs/AgNs SERS-active substrates were observed in this study. OriginPro 8.5 software was used for background subtraction of the Raman spectra. Baseline correction was performed by plotting the graph in OriginPro software (ver. 8.5, Shopee, Selangor, Malaysia) and then using the peak analyser function to remove the background. Absorption spectra and the structure of colloidal AuNs, AgNs and AuNs/AgNs were recorded using a UV-2600 Shimadzu spectrometer and a Hitachi HT7700 120-kV TEM. The combination of gold and silver elements in the colloid phase was determined using EDS and STEM analysis using a Hitachi HT7700 120-kV TEM. AuNs, AgNs and AuNs/AgNs thin film surfaces were characterised using a UV-2600 Shimadzu spectrometer and a JEOL JSM-7100F FESEM.

Ethics

This work does not contain any studies involving human participants or animals performed by the authors.

Supplementary material

Supplementary material is available [online](#).

References

- Savary S, Willocquet L, Pethybridge SJ, Esker P, McRoberts N, Nelson A. The global burden of pathogens and pests on major food crops. *Nat Ecol Evol* 2019; 3: 430–439. doi:10.1038/s41559-018-0793-y
- Tomizawa M, Casida JE. Neonicotinoid insecticide toxicology: mechanisms of selective action. *Annu Rev Pharmacol Toxicol* 2005; 45: 247–268. doi:10.1146/annurev.pharmtox.45.120403.095930
- Zhang C, Tian D, Yi X, Zhang T, Ruan J, Wu R, Chen C, Huang M, Ying G. Occurrence, distribution and seasonal variation of five neonicotinoid insecticides in surface water and sediment of the Pearl Rivers, South China. *Chemosphere* 2019; 217: 437–446. doi:10.1016/j.chemosphere.2018.11.024
- Hladik ML, Kolpin DW. First national-scale reconnaissance of neonicotinoid insecticides in streams across the USA. *Environ Chem* 2016; 13: 12–20. doi:10.1071/EN15061
- Hashimoto F, Takanashi H, Nakajima T, Ueda T, Kadokawa J, Ishikawa H, Miyamoto N. Occurrence of imidacloprid and its transformation product (imidacloprid-nitroguanidine) in rivers during an irrigating and soil puddling duration. *Microchem J* 2020; 153: 104496. doi:10.1016/j.microc.2019.104496
- Wei X, Pan Y, Tang Z, Lin Q, Jiang Y, Chen J, Xian W, Yin R, Li AJ, Qiu R. Neonicotinoids residues in cow milk and health risks to the Chinese general population. *J Hazard Mater* 2023; 452: 131296. doi:10.1016/j.jhazmat.2023.131296
- Xu T, Xu QG, Li H, Wang J, Li QX, Shelver WL, Li J. Strip-based immunoassay for the simultaneous detection of the neonicotinoid insecticides imidacloprid and thiamethoxam in agricultural products. *Talanta* 2012; 101: 85–90. doi:10.1016/j.talanta.2012.08.047
- Camargo PH, Au L, Rycenga M, Li W, Xia Y. Measuring the SERS enhancement factors of dimers with different structures constructed from silver nanocubes. *Chem Phys Lett* 2010; 484: 304–308. doi:10.1016/j.cplett.2009.12.002
- Shoute LCT. Multilayer substrate-mediated tuning resonance of plasmon and SERS EF of nanostructured silver. *ChemPhysChem* 2010; 11: 2539–2545. doi:10.1002/cphc.201000351
- Deng J, Dong J, Cohen P. Rapid Fabrication and Characterization of SERS Substrates. *Procedia Manuf* 2018; 26: 580–586. doi:10.1016/j.promfg.2018.07.068
- Sitjar J, Liao J-D, Lee H, Liu BH, Fu W-e. SERS-active substrate with collective amplification design for trace analysis of pesticides. *Nanomaterials* 2019; 9: 664. doi:10.3390/nano9050664
- Ngo TC, Trinh QT, Thi Thai An N, Tri NN, Trung NT, Truong DH, Huy BT, Nguyen MT, Dao DQ. SERS spectra of the pesticide chlorpyrifos adsorbed on silver nanosurface: the Ag₂₀ cluster model. *J Phys Chem C* 2020; 124: 21702–21716. doi:10.1021/acs.jpcc.0c06078
- Vinnacombe-Willson GA, Conti Y, Jonas SJ, Weiss PS, Mihi A, Scarabelli L. Surface lattice plasmon resonances by direct *in situ* substrate growth of gold nanoparticles in ordered arrays. *Adv Mater* 2022; 34: 2205330. doi:10.1002/adma.202205330
- Mehmandoust S, Sahbafar H, Mohsennezhad A, Hadi A, Eskandari V. Experimental and numerical evaluations of flexible filter paper substrates for sensitive and rapid identification of methyl parathion pesticide via surface-enhanced Raman scattering (SERS). *Vib Spectrosc* 2023; 129: 103586. doi:10.1016/j.vibspec.2023.103586
- Azar İ, Kumral NA. Validation of LC-MS/MS method for simultaneous determination of chlorpyrifos, deltamethrin, imidacloprid and some of their metabolites in maize silage. *J Environ Sci Heal Part B* 2022; 57: 125–132. doi:10.1080/03601234.2022.2029275
- Mozzaquatro JdO, César IA, Pinheiro AEB, Caldas ED. Pesticide residues analysis in passion fruit and its processed products by LC-MS/MS and GC-MS/MS: method validation, processing factors and dietary risk assessment. *Food Chem* 2022; 375: 131643. doi:10.1016/j.foodchem.2021.131643
- Quan Z, Li H, Sun S, Xu Y. Research process in application of fluorescent sensor for pesticide detection. *Adv Agrochem* 2023; 2: 107–112. doi:10.1016/j.aac.2023.02.003
- Yin X, Li H, Wu S, Lu Y, Yang Y, Qin L, Li L, Xiao J, Liang J, Si Y, Le T, Peng D. A sensitive and specific enzyme-linked immunosorbent assay for the detection of pymetrozine in vegetable, cereal, and meat. *Food Chem* 2023; 418: 135949. doi:10.1016/j.foodchem.2023.135949
- Sánchez-Hernández L, Hernández-Domínguez D, Bernal J, Neusüß C, Martín MT, Bernal JL. Capillary electrophoresis–mass spectrometry as a new approach to analyze neonicotinoid insecticides. *J Chromatogr A* 2014; 1359: 317–324. doi:10.1016/j.chroma.2014.07.028
- Hu Y, Cheng H, Zhao X, Wu J, Muhammad F, Lin S, He J, Zhou L, Zhang C, Deng Y, Wang P, Zhou Z, Nie S, Wei H. Surface-enhanced Raman scattering active gold nanoparticles with enzyme-mimicking activities for measuring glucose and lactate in living tissues. *ACS Nano* 2017; 11: 5558–5566. doi:10.1021/acsnano.7b00905
- Truc Phuong NT, Dang VQ, Van Hieu L, Bach TN, Khuyen BX, Thi Ta HK, Ju H, Phan BT, Thi Tran NH. Functionalized silver nanoparticles for SERS amplification with enhanced reproducibility and for ultrasensitive optical fiber sensing in environmental and biochemical assays. *RSC Adv* 2022; 12: 31352–31362. doi:10.1039/D2RA06074D
- Cui Y, Ren B, Yao J-L, Gu R-A, Tian Z-Q. Synthesis of Ag_{core}Au_{shell} bimetallic nanoparticles for immunoassay based on surface-enhanced Raman spectroscopy. *J Phys Chem B* 2006; 110: 4002–4006. doi:10.1021/jp056203x
- Sivanesan A, Witkowska E, Adamkiewicz W, Dziewit Ł, Kamińska A, Waluk J. Nanostructured silver–gold bimetallic SERS substrates for selective identification of bacteria in human blood. *Analyst* 2014; 139: 1037–1043. doi:10.1039/C3AN01924A

- 24 de Puig H, Tam JO, Yen C-W, Gehrke L, Hamad-Schifferli K. Extinction coefficient of gold nanostars. *J Phys Chem C* 2015; 119: 17408–17415. doi:10.1021/acs.jpcc.5b03624
- 25 Paramelle D, Sadovoy A, Gorelik S, Free P, Hoblely J, Fernig DG. A rapid method to estimate the concentration of citrate capped silver nanoparticles from UV-visible light spectra. *Analyst* 2014; 139: 4855–4861. doi:10.1039/C4AN00978A
- 26 Hou R, Pang S, He L. *In situ* SERS detection of multi-class insecticides on plant surfaces. *Anal Methods* 2015; 7: 6325–6330. doi:10.1039/C5AY01058F
- 27 Zhang H, Kang Y, Liu P, Tao X, Pei J, Li H, Du Y. Determination of pesticides by surface-enhanced Raman spectroscopy on gold-nanoparticle-modified polymethacrylate. *Anal Lett* 2016; 49: 2268–2278. doi:10.1080/00032719.2016.1147577
- 28 Chen Q, Hassan MM, Xu J, Zareef M, Li H, Xu Y, Wang P, Agyekum AA, Kutsanedzie FYH, Viswadevarayalu A. Fast sensing of imidacloprid residue in tea using surface-enhanced Raman scattering by comparative multivariate calibration. *Spectrochim Acta Part A Mol Biomol Spectrosc* 2019; 211: 86–93. doi:10.1016/j.saa.2018.11.041
- 29 Zhu A, Xu Y, Ali S, Ouyang Q, Chen Q. Au@Ag nanoflowers based SERS coupled chemometric algorithms for determination of organochlorine pesticides in milk. *LWT* 2021; 150: 111978. doi:10.1016/j.lwt.2021.111978
- 30 Creedon N, Lovera P, Moreno JG, Nolan M, O’Riordan A. Highly sensitive SERS detection of neonicotinoid pesticides. Complete Raman spectral assignment of clothianidin and imidacloprid. *J Phys Chem A* 2020; 124: 7238–7247. doi:10.1021/acs.jpca.0c02832
- 31 Al-Syadi AM, Faisal M, Harraz FA, Jalalah M, Alsaiani M. Immersion-plated palladium nanoparticles onto meso-porous silicon layer as novel SERS substrate for sensitive detection of imidacloprid pesticide. *Sci Rep* 2021; 11: 9174. doi:10.1038/s41598-021-88326-0
- 32 Atanasov PA, Nedyalkov NN, Fukata N, Jevasuwan W, Subramani T. Surface-enhanced Raman spectroscopy of neonicotinoid insecticide imidacloprid, assisted by gold and silver nanostructures. *Spectrosc Lett* 2020; 53: 184–193. doi:10.1080/00387010.2020.1726400
- 33 Pan F, Wu H, Tang J, Xiang L, Wei J. Sensitive detection of imidacloprid at ultra-trace level utilizing ratiometric surface-enhanced Raman scattering platform based on C₆₀ and rhodamine 6G. *Chem Pap* 2022; 76: 5571–5578. doi:10.1007/s11696-022-02263-4
- 34 Batmunkh M, Macdonald TJ, Peveler WJ, Bati ASR, Carmalt CJ, Parkin IP, Shapter JG. Plasmonic gold nanostars incorporated into high-efficiency perovskite solar cells. *ChemSusChem* 2017; 10: 3750–3753. doi:10.1002/cssc.201701056
- 35 Abu Bakar N, Shapter JG. Silver nanostar films for surface-enhanced Raman spectroscopy (SERS) of the pesticide imidacloprid. *Heliyon* 2023; 9: e14686. doi:10.1016/j.heliyon.2023.e14686

Data availability. Data will be made available on request.

Conflicts of interest. The authors declare that they have no conflicts of interest.

Declaration of funding. Joseph George Shapter was supported by the Australian Research Council (DP200101217). Norhayati Abu Bakar received a post-doctoral fellowship from the Ministry of Higher Education Malaysia and Universiti Kebangsaan Malaysia.

Acknowledgements. Norhayati Abu Bakar thanks the Ministry of Higher Education Malaysia and Universiti Kebangsaan Malaysia for her fellowship. The characterisation work was supported by the Centre for Microscopy and Microanalysis (CMM), University of Queensland, Australia. This work was performed in part at the Queensland node of the Australian National Fabrication Facility, a company established under the National Collaborative Research Infrastructure Strategy to provide nano- and micro-fabrication facilities for Australia’s researchers.

Author affiliations

^AAustralian Institute for Bioengineering and Nanotechnology, University of Queensland, Saint Lucia, Brisbane, Qld 4072, Australia.

^BInstitute of Microengineering and Nanoelectronic, Universiti Kebangsaan Malaysia, UKM Bangi, 43600, Bangi, Selangor, Malaysia.